

Barrier Inhomogeneity of Ni Schottky Contacts to Bulk GaN

Giuseppe Greco, Filippo Giannazzo, Patrick Fiorenza, Salvatore Di Franco, Alessandra Alberti, Ferdinando Iucolano, Ildiko Cora, Bela Pecz, and Fabrizio Roccaforte*

Gallium nitride (GaN) is a promising candidate for high-power and high-frequency devices. To date, the lack of large area bulk GaN materials of reasonable cost and quality has limited the technology almost completely to lateral devices. However, vertical structures are attractive to obtain a higher current density and a reduced device size. In this work, the electrical behavior of a Ni/Au Schottky barrier on bulk GaN material is studied, using vertical Schottky diodes. The forward current–voltage characteristics of the diodes reveal a temperature dependence of both the ideality factor (n) and of the Schottky barrier height (Φ_B). The ideal value of the barrier of 1.72 eV extrapolated at $n = 1$ is in agreement with the results obtained by capacitance–voltage measurements. A nanoscale electrical analysis performed by conductive atomic force microscopy (C-AFM) allow to visualize the barrier height inhomogeneity and to correlate the current distribution to the surface morphology of the material. The barrier inhomogeneity explains the temperature behavior of ideality factor and barrier height determined by the macroscopic diodes. Preliminary structural analyses carried out by transmission electron microscopy (TEM) of the metal semiconductor interface revealed a typically flat Au/Ni bilayer structure, the Ni layer being epitaxial to GaN, with some mosaicity.

1. Introduction

Since more than two decades, Gallium Nitride (GaN) and related materials have been object of intensive investigations, which are mainly finalized to the potential applications in the fields of optoelectronics, high-power and high-frequency devices.^[1–3]

In principle, due to its larger band gap (3.4 eV) and higher critical field (expected in the range of 3.60–3.75 MV cm^{−1}),^[4] the figure of merits of GaN for power devices should be even superior than those of the other well-established wide band gap semiconductor, silicon carbide (SiC).^[5] However, while high voltage SiC Schottky diodes and metal-oxide-semiconductor field effect transistors (MOSFETs) are already available in the market,^[6] to date the commercialization of GaN power devices has been delayed by several materials and processing issues.^[7,8]

As an example, one of the main limits for the applications of GaN-based materials in power devices has been represented by the need of growing GaN on lattice-

mismatched substrates (such as sapphire, silicon, or SiC), which typically result in high defect density, poor quality of the material (excess of leakage, premature breakdown, etc.).


Now, after a decade of rapid progress in epitaxial growth and devices processing technology, large area GaN-on-Si heterostructures are available and power devices with excellent efficiency and compact size start to be implemented.^[9,10] However, for power electronics applications, fabricating semiconductor devices on bulk GaN substrates would be desired, to fully exploit the true electric field strength, and to create vertical architectures, with higher current density and reduced device size, which are not affected from reliability issues associated with the near-surface conduction.^[11]

In the last decade, a variety of devices operating at high-voltage and high current levels, with low specific on-resistance (e.g., Schottky diodes,^[12,13] vertical MOSFETs,^[14–16] vertical transistors based on AlGaIn/GaN heterostructures,^[17,18] and p–n junctions^[19,20]) have been reported on bulk GaN substrates. Recently, Ni-based Schottky barrier devices (diodes and transistors) with low leakage current have been demonstrated

Dr. G. Greco, Dr. F. Giannazzo, Dr. P. Fiorenza, Dr. S. Di Franco, Dr. A. Alberti, Dr. F. Roccaforte
Consiglio Nazionale delle Ricerche – Istituto per la Microelettronica e Microsistemi (CNR-IMM)
Strada VIII, n. 5 Zona Industriale,
95121 Catania, Italy
E-mail: fabrizio.roccaforte@imm.cnr.it

Dr. F. Iucolano
STMicrolithronics
Stradale Primrose 50, 95121 Catania, Italy

Dr. I. Cora, Dr. B. Pecz
Centre for Energy Research Institute for Technical Physics and Materials Science
Hungarian Academy of Sciences
P.O. Box 49, 1525 Budapest, Hungary

 The ORCID identification number(s) for the author(s) of this article can be found under <https://doi.org/10.1002/pssa.201700613>.

DOI: 10.1002/pssa.201700613

on high-quality AlGaIn/GaN heterostructures grown on amorphous bulk GaN substrates.^[21]

Among the aforementioned devices structures, Schottky diodes can lead to significant benefits when replacing silicon-based fast rectifiers in switching applications, such as power factor correction (PFC).^[22]

The main building block of such devices is the metal/semiconductor contact, whose properties and uniformity strongly depend on the material quality and surface preparation and, ultimately, affect the device performances.

Hence, the knowledge of the electrical behavior of metal/GaN Schottky contacts is a fundamental topic.

Metal/semiconductor Schottky barriers have been widely investigated on n-type GaN in the last two decades.^[23–28] In general, the classical thermionic emission (TE) or thermionic field emission (TFE) models have been used to describe the transport mechanisms at metal/GaN interfaces from the temperature dependence of Schottky diodes characteristics.^[29–34] Moreover, the role of surface processing,^[35,36] post-annealing conditions,^[37] and of material defects^[31,38–40] has been widely discussed.

In this context, the combination of macroscopic electrical measurements on conventional Schottky contacts with local nanoscale electrical analyses has been demonstrated to be a promising approach to assess the fundamental parameters of the barrier and predict the temperature behavior of the forward current.^[41]

In this paper, the electrical behavior of a Ni/Au Schottky barrier on bulk GaN was studied by a combination of conventional macroscopic measurements on vertical Schottky diodes with nanoscale analyses performed by conductive atomic force microscopy (C-AFM). The temperature-dependent I - V characteristics in forward bias suggested the formation of an inhomogeneous Schottky barrier. The barrier inhomogeneity could be visualized by the local current distribution obtained by C-AFM.

2. Experimental Section

The experiments were carried on commercial material, i.e., 3 μm thick n-type GaN epitaxial layer, with a nominal doping concentration of $1 \times 10^{16} \text{ cm}^{-3}$, grown onto heavily doped ($N_D = 1\text{--}5 \times 10^{18} \text{ cm}^{-3}$) GaN substrates. The GaN substrate was grown by hydride vapor phase epitaxy (HVPE), while metal-organic chemical vapor phase epitaxy (MOVPE) has been used to grow the epitaxial layer. The off-cut angle was 0.4° . High resolution X-ray diffraction analyses has been performed using a D8Discover made by Bruker AXS to get insights into the material quality. In particular, measuring the FWHM for the (0002), (0004), and (0006) peaks and following the procedure reported by Heinke et al.^[42] allowed us estimating a screw dislocation density in the range of $4\text{--}5 \times 10^7 \text{ cm}^{-2}$.

As a first step, a 800 nm silicon dioxide (SiO_2) hard mask has been deposited on the sample front-side by a low-temperature plasma enhanced chemical vapor deposition process,^[43] in order to keep protected the surface during the device processing. Then, a large area Ohmic contact was created on the wafer back-side by the deposition of a $\text{Ti}_{(15 \text{ nm})}/\text{Al}_{(200 \text{ nm})}/\text{Ni}_{(50 \text{ nm})}/\text{Au}_{(50 \text{ nm})}$

multilayer, followed by an annealing at 750°C .^[44] In order to form the Schottky contact on the front-side of the wafer, the SiO_2 hard mask was removed by wet etch in buffered hydrofluoric solution, just immediately before depositing a sequence $\text{Ni}_{(100 \text{ nm})}/\text{Au}_{(100 \text{ nm})}$ bilayer.^[45]

The circular Schottky diodes have been defined by standard lithography and sequential wet-etch of the Ni/Au bilayer.

The thermal annealing processes of Schottky and Ohmic contacts have been carried out in argon atmosphere, using a JIPELEC JetFirst 150 furnace.

Nanoscale resolution morphological and electrical characterization of the bare GaN surface was performed by conductive atomic force microscopy (C-AFM) using a DI3100 equipment with Nanoscope V controller electronics. This analysis was carried out before the Schottky contact deposition, i.e., after the wet etch of the SiO_2 layer. Doped diamond coated Si tips were used for local electrical measurements, as they ensure a stable electrical contact during long time scans even on rough surfaces. Moreover, the microstructure of the metal/semiconductor contact was monitored also by means of cross section transmission electron microscopy (TEM), using a JEOL 3010 microscope operating at 300 kV.

3. Results and Discussion

A schematic of the fabricated vertical Schottky diodes is shown in **Figure 1**. On these diodes, the forward I - V characteristics were acquired at different temperatures, in the range $25\text{--}150^\circ\text{C}$. A representative temperature dependence of the forward I - V curves is reported in a semilog plot in **Figure 2**. As can be seen, two regions can be distinguished in the I - V curves: (i) at low bias values ($V_F < 1 \text{ V}$) the I - V curves are linear and the forward current increases with increasing the measurement temperature; (ii) at higher bias values ($V_F > 1 \text{ V}$) the current approximately follows the opposite trend, i.e., it decreases with increasing the temperature. This is due to the fact that at low bias the current transport is dominated by the thermionic emission mechanism, while at higher bias values the series

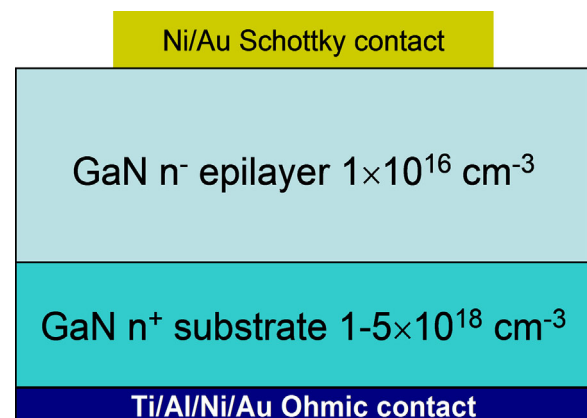


Figure 1. Schematic of the fabricated vertical Schottky diode on bulk GaN epitaxial layers. The nominal values/range of the epilayer and substrate doping given by the supplier are also reported.

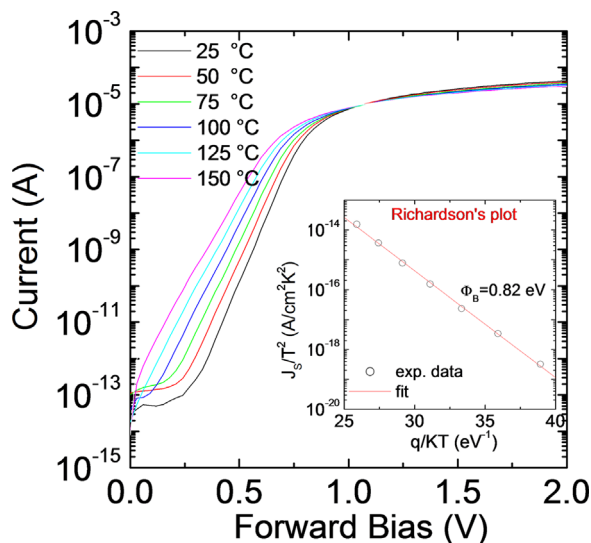


Figure 2. Forward I - V characteristics of the fabricated Schottky diodes, acquired in the temperature range between 25 and 150 °C. The inset shows the Richardson's plot.

resistance becomes dominant and the current decreases with increasing the temperature.^[46]

The linear region of the forward I - V curve can be fitted using the thermionic emission (TE) model, i.e., using the equation:

$$I = A J_s \exp\left(\frac{q V_F}{n k_B T}\right) \quad (1)$$

$$\text{with } J_s = A^* T^2 \exp\left(\frac{-q \Phi_B}{k_B T}\right) \quad (2)$$

and where A is the diode area ($3.14 \times 10^{-4} \text{ cm}^2$), A^* is the Richardson's constant of GaN ($26.9 \text{ A cm}^{-2} \text{ K}^{-2}$),^[47] k_B is the Boltzmann constant, q is the elementary charge, T the absolute temperature, n is the ideality factor, and Φ_B is the Schottky barrier height.

Moreover, from the reverse saturation current J_s acquired at each temperature, the Richardson's plot could be extracted, as shown in the inset of Figure 2. From the fit of the experimental data of this plot an effective barrier height of 0.82 eV has been estimated.

On the other hand, **Figure 3a** reports the ideality factor n and the Schottky barrier height Φ_B , extracted by the linear fit done applying the TE model (Eq. (1)), as a function of the temperature T . Evidently, the ideality factor n decreases from 1.18 at room temperature down to 1.13 at 150 °C. On the other hand, the values of the barrier height Φ_B increase in the same range from 1.18 eV (at room temperature) to 1.33 eV (at 150 °C). This behavior is typical of an inhomogeneous barrier^[48] and is similar to what has been already observed in Schottky contacts to GaN.^[40,41] Also the discrepancy between the effective barrier height determined by the Richardson's plot and the values determined by the linear fit of the I - V curve using the TE theory is fully consistent with the occurrence of an inhomogeneous barrier.^[48]

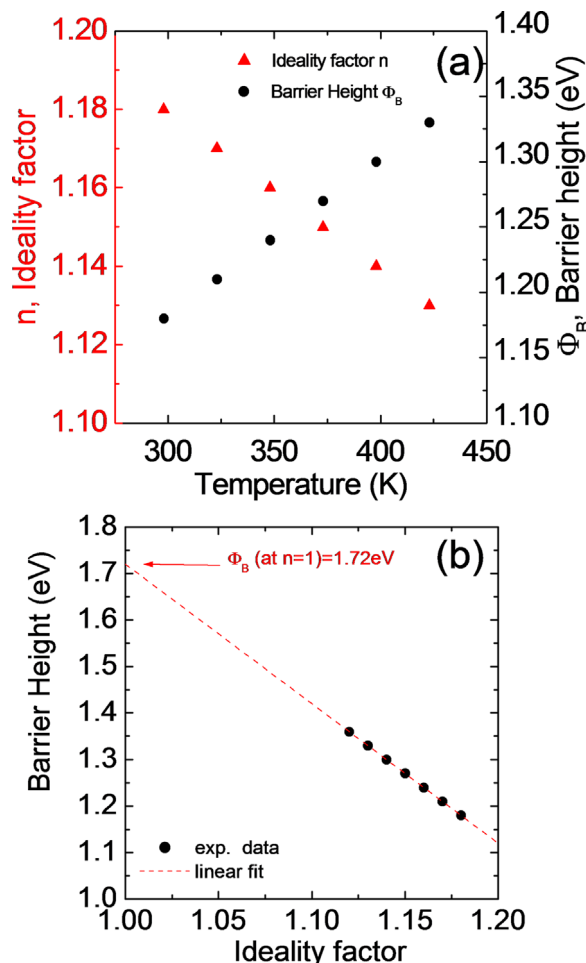


Figure 3. a) Ideality factor n and Schottky barrier height Φ_B as a function of the temperature T , determined from the linear fit of the forward I - V curves shown in Figure 2, applying the thermionic emission model; (b) Schottky barrier height Φ_B as a function of the ideality factor n ; the extrapolation at $n = 1$ (ideal case) gives a value of the ideal barrier of 1.72 eV.

It is worth noting that the Schottky barrier height measured at different temperatures and the corresponding ideality factor values are correlated, as can be clearly seen by the plot reported in Figure 3b. In particular, by a linear fit of the data it was possible to extrapolate the value of the barrier height Φ_B in the ideal case (at $n = 1$) of 1.72 eV.

Capacitance-voltage (C - V) measurements performed on the Schottky diodes under reverse bias. The $1/C^2$ curve is reported in **Figure 4** as a function of the bias. The inset shows the C - V curve: from a linear fit of the $1/C^2$ curve it was possible to extract a value of the barrier height of 1.72 eV, which is the same as the one extrapolated from the plot in Figure 3b. Moreover, the value of the epilayer doping extracted by this analysis (from slope of the linear fit) was $4 \times 10^{15} \text{ cm}^{-3}$, i.e., lower than the nominal doping level provided by the material supplier. Clearly, for small positive bias values the C - V curve dramatically drops down (inset of Figure 4), as a consequence of the increased conductance of the diode.

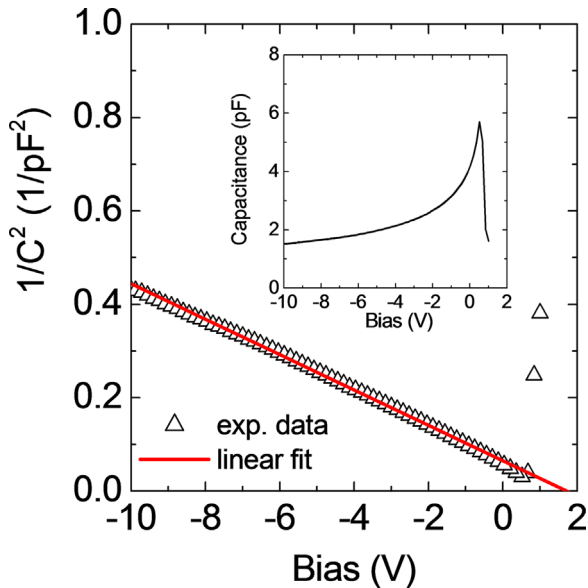


Figure 4. Plot of $1/C^2$ as a function of the bias for the Ni/GaN Schottky diodes. The inset shows the C - V curve. A doping level of $4 \times 10^{15} \text{ cm}^{-3}$ and a barrier height of 1.72 eV were extracted from the slope and x-axis intercept of the linear fit of the $1/C^2$ curve.

In order to get additional physical insights into the Schottky barrier inhomogeneity, morphological and current measurements were acquired on the sample surface by means of C-AFM. The surface morphology was inspected by scanning the conductive tip in contact mode on a the bare GaN surface. A current map was acquired simultaneously, by applying a positive bias between the tip and the macroscopic Ohmic back-contact and measuring the current flowing vertically between these two contacts with a current sensor connected in series to the tip (see schematic in **Figure 5a**). In this configuration, for each position on GaN surface, the tip contact resembles a nanoscale Schottky diode under forward bias polarization.^[49]

The morphological image in **Figure 5b** exhibits characteristic protrusions (hillocks), resulting in a high value of the root mean square (RMS) roughness (27.3 nm). Interestingly, a correlation between most of the surface regions showing these hillocks with highly conductive areas in the current map can be observed.

As can be deduced from the schematic in **Figure 5a**, the locally measured front-to-back current is the result of different resistance contributions in series, i.e., the tip/GaN contact resistance R_c , the spreading resistance R_{spr} associated to current spreading from the nanoscale tip contact to the epilayer, the series resistance of the n^- -GaN epilayer (R_{s_epi}) and of the n^- -GaN substrate (R_{s_sub}), and the resistance of the Ohmic back-contact (R_{c_back}). However, among these resistive terms, only R_c and R_{spr} typically contain local information on the electrical properties of the semiconductor material in the near-surface region, whereas the other terms contribute to determine the average current level measured in the from-to-back analyses.

The preferential current injection in the GaN areas showing hillocks, visible in the current map in **Figure 5c**, is fully consistent with the formation of a lower Schottky barrier on these surface protrusions with respect to the planar GaN regions.

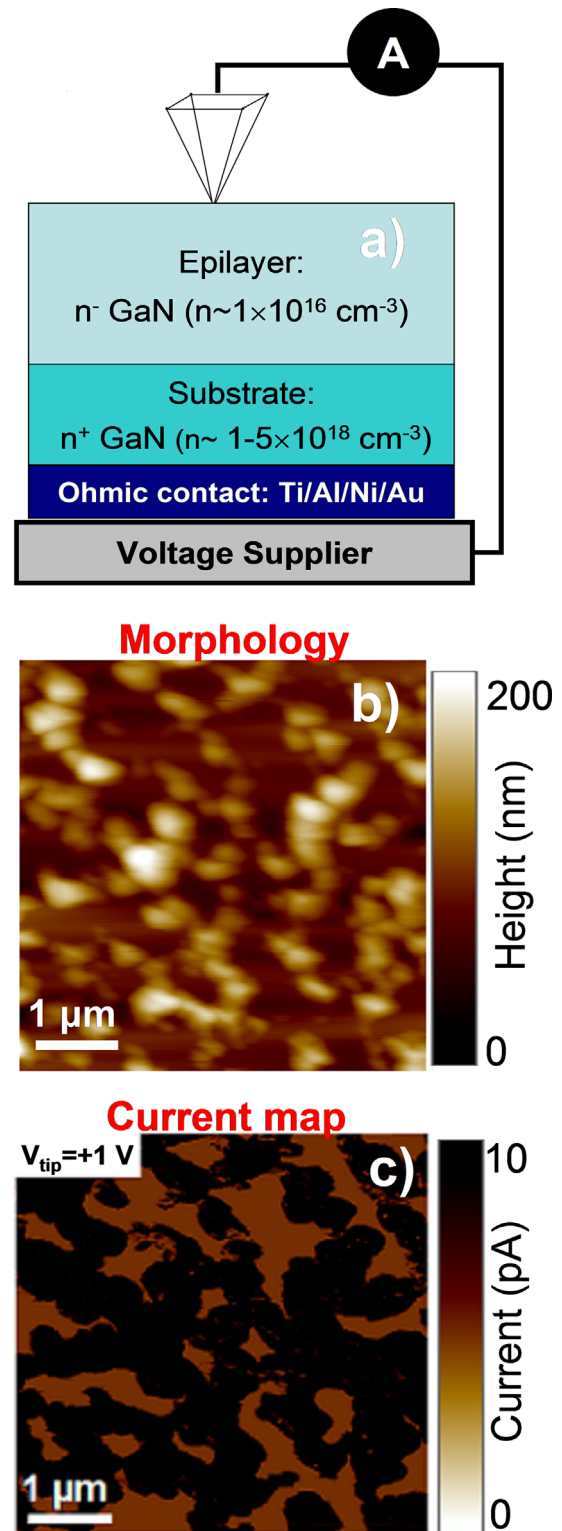


Figure 5. a) Schematic of the experimental set-up used to perform the C-AFM measurement, b) AFM image of the surface morphology of the GaN epilayer; c) current map acquired by C-AFM.

Hence, nanoscale current mapping indicates that micrometer size inhomogeneities related to the GaN surface morphology can be one of the sources of the inhomogeneous Schottky barrier behavior deduced from temperature dependent electrical characterization of macroscopic Schottky contacts. Similarly, Ren et al.^[50] pointed out that the ideality factor of Schottky contacts on bulk GaN can be significantly improved by the optimizing growth conditions and, hence, the surface morphology of the epilayer.

However, it cannot be ruled out that the presence of residual contaminations from the processing contribute to the high values of barrier height determined by C - V analysis. As matter of fact, Reddy et al.^[51] investigated the possibility to improve the temperature stability and the barrier homogeneity by appropriate surface treatment. In particular, they pointed out that the removal of additional surface phases or defects introduced during development is essential to obtain an ideality behavior and an homogenous barrier.

The microstructure of the metal/semiconductor contact was evaluated by means of cross section TEM images. **Figure 6** shows the typical situation observed at the metal/GaN interface. As can be seen, flat surface and interface of the Au/Ni bilayer structure are observed. Preliminary selective area diffraction patterns (not shown here), acquired in this region at the Ni/GaN interface, indicated that Ni is mostly epitaxially oriented with respect to the GaN substrate, according to the relation $Ni(111)/GaN(0001)$,^[52] although it exhibits some mosaicity. Moreover, no interlayer was observed between the substrate and the contact layer. The grain size of Ni and Au is in the 100 nm range.

In other regions along the metal film, also some bumps of the Au layer have been observed on the underlying flat and homogeneous Ni layer. This evidence can be associated with the morphological features observed on the sample surface by AFM. However, further structural analyses of the interface are needed to have a more clear scenario and establish a better correlation with the electrical behavior.

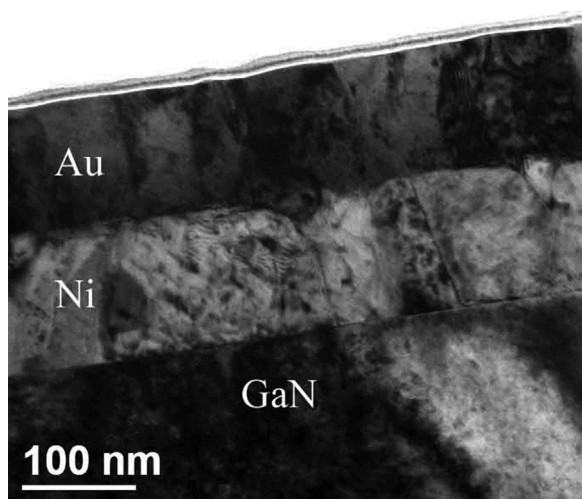


Figure 6. Cross section TEM image of the Au/Ni/GaN Schottky interface.

4. Conclusions

In this paper, the electrical behavior of vertical Schottky diodes on bulk GaN material has been studied by a combination of temperature dependent I - V measurements and nanoscale local current measurements by C-AFM. The forward current-voltage characteristics of the diodes revealed a temperature dependence of ideality factor and Schottky barrier height. This behavior is indicative of the occurrence of an inhomogeneous barrier. The nanoscale electrical analysis performed by C-AFM allowed to directly monitor the barrier height inhomogeneity and to correlate the current distribution to the surface morphology of the material. The barrier inhomogeneity explains the temperature behavior of ideality factor and barrier height determined by the macroscopic diodes. The results are useful to predict the temperature-dependent device behavior and point out the importance of the epilayer surface to optimize the barrier height homogeneity.

Acknowledgments

Part of this work has been carried out in the framework of the project GHOST, within the collaboration agreement between CNR and HAS 2016–2018. The authors would like to acknowledge S. Reina and A. Parisi from STMicroelectronics for the technical support during electrical measurements. B. P. and I. C. thank the financial support of the OTKA 108869 project.

Conflict of Interest

The authors declare no conflict of interest.

Keywords

bulk GaN, Ni/Au, Schottky barrier

Received: August 23, 2017

Revised: November 9, 2017

Published online:

- [1] F. Ren, J. C. Zolper, *Wide Band Gap Electronic Devices*. World Scientific, Singapore **2003**.
- [2] R. Quai, *Gallium Nitride Electronics*. Springer Verlag, Berlin Heidelberg **2008**.
- [3] M. Meneghini, G. Meneghesso, E. Zanoni, *Power GaN Devices – Materials, Applications and Reliability*. Springer International Publishing Switzerland, Cham (ZG)Switzerland **2017**.
- [4] I. C. Kizilyalli, A. P. Edwards, H. Nie, D. Disney, D. Bour, *IEEE Trans. Electron Devices* **2013**, 60, 3067.
- [5] F. Roccaforte, P. Fiorenza, G. Greco, R. Lo Nigro, F. Giannazzo, A. Patti, M. Saggio, *Phys. Status Solidi a* **2014**, 211, 2063.
- [6] T. Kimoto, *Jap. J. Appl. Phys.* **2015**, 54, 040103.
- [7] F. Roccaforte, F. Giannazzo, F. Lucolano, J. Eriksson, M. H. Weng, V. Raineri, *Appl. Surf. Sci.* **2010**, 256, 5727.
- [8] F. Roccaforte, P. Fiorenza, G. Greco, M. Vivona, R. Lo Nigro, F. Giannazzo, A. Patti, M. Saggio, *Appl. Surf. Sci.* **2014**, 301, 9.
- [9] S. Tripathy, V. K. X. Lin, S. B. Dolmanan, J. P. Y. Tan, R. S. Kajen, L. K. Bera, S. L. Teo, M. K. Kumar, S. Arulkumaran, G. I. Ng, S. Vicknesh, S. Todd, W. Z. Wang, G. Q. Lo, H. Li, D. Lee, S. Han, *Appl. Phys. Lett.* **2012**, 101, 082110.

- [10] K. J. Chen, O. Häberlen, A. Lidow, C. I. Tsai, T. Ueda, Y. Uemoto, Y. Wu, *IEEE Trans. Electron Devices* **2017**, *64*, 779.
- [11] I. C. Kizilyalli, P. Bui-Quanga, D. Disney, H. Bhatia, O. Aktas, *Microelectron. Reliab.* **2015**, *55*, 1654.
- [12] Y. Wang, H. Xu, S. Alur, Y. Sharma, F. Tong, P. Gartland, T. Issacs-Smith, C. Ahyi, J. Williams, M. Park, G. Wheeler, M. Johnson, A. A. Allerman, A. Hanser, T. Paskova, E. A. Preble, K. R. Evans, *Phys. Status Solidi C* **2011**, *8*, 2430.
- [13] N. Tanaka, K. Hasegawa, K. Yasunishi, N. Murakami, T. Oka, *Appl. Phys. Express* **2015**, *8*, 071001.
- [14] H. Otake, K. Chikamatsu, A. Yamaguchi, T. Fujishima, H. Ohta, *Appl. Phys. Express* **2008**, *1*, 011105.
- [15] M. Kodama, *Appl. Phys. Express* **2008**, *1*, 021104.
- [16] T. Oka, Y. Ueno, T. Ina, K. Hasegawa, *Appl. Phys. Express* **2014**, *7*, 021002.
- [17] S. Chowdhury, B. L. Swenson, M. H. Wong, U. K. Mishra, *Semicond. Sci. Technol.* **2013**, *28*, 074014.
- [18] H. Nie, Q. Diduck, B. Alvarez, A. P. Edwards, B. M. Kayes, M. Zhang, G. Ye, T. Prunty, D. Bour, I. C. Kizilyalli, *IEEE Electron Devices Lett.* **2014**, *35*, 939.
- [19] I. C. Kizilyalli, A. P. Edwards, H. Nie, D. Disney, D. Bour, *IEEE Trans. Electron Dev.* **2013**, *60*, 3067.
- [20] Z. Hu, K. Nomoto, B. Song, M. Zhu, M. Qi, M. Pan, X. Gao, V. Protasenko, D. Jena, H. G. Xing, *Appl. Phys. Lett.* **2015**, *107*, 243501.
- [21] P. Kruszewski, P. Prystawko, I. Kasalynas, A. Nowakowska-Siwinska, M. Krysko, J. Plesiewicz, J. Smalc-Koziorowska, R. Dwilinski, M. Zajac, R. Kucharski, M. Leszczynski, *Semicond. Sci. Technol.* **2014**, *29*, 075004.
- [22] D. Alquier, F. Cayrel, O. Menard, A. E. Bazin, A. Yvon, E. Collard, *Jap. J. Appl. Phys.* **2012**, *51*, 01AG08.
- [23] J. D. Guo, F. M. Pan, M. S. Feng, R. J. Guo, P. F. Chou, C. Y. Chang, *J. Appl. Phys.* **1996**, *80*, 1623.
- [24] T. U. Kampen, W. Mönch, *Appl. Surf. Sci.* **1997**, *117–118*, 288.
- [25] P. Hacke, T. Detchprohm, K. Hiramatsu, N. Sawaki, *Appl. Phys. Lett.* **2003**, *63*, 2676.
- [26] J. K. Kim, H. W. Jang, J. L. Lee, *J. Appl. Phys.* **2003**, *94*, 7201.
- [27] C. Lu, S. Noor Mohammad, *Appl. Phys. Lett.* **2006**, *89*, 162111.
- [28] F. Roccaforte, F. Giannazzo, F. Iucolano, J. Eriksson, M. H. Weng, V. Raineri, *Appl. Surf. Sci.* **2010**, *256*, 5727 and references therein.
- [29] L. S. Yu, Q. Z. Liu, Q. J. Xing, D. J. Qiao, S. S. Lau, J. Redwing, *J. Appl. Phys.* **1998**, *84*, 2099.
- [30] J. Kotani, T. Hashizume, H. Hasegawa, *J. Vac. Sci. Technol. B* **2004**, *22*, 2179.
- [31] A. R. Arehart, B. Moran, J. S. Speck, U. K. Mishra, S. P. DenBaars, S. A. Ringela, *J. Appl. Phys.* **2006**, *100*, 023709.
- [32] Y. Zhou, D. Wang, C. Ahyi, C.-C. Tin, J. Williams, M. Parka, N. M. Williams, A. Hanser, E. A. Preble, *J. Appl. Phys.* **2007**, *101*, 024506.
- [33] Y.-J. Lin, *J. Appl. Phys.* **2009**, *106*, 013702.
- [34] Y. Wang, S. Alur, Y. Sharma, F. Tong, R. Thapa, P. Gartland, T. Issacs-Smith, C. Ahyi, J. Williams, M. Park, M. Johnson, T. Paskova, E. A. Preble, K. R. Evans, *Semicond. Sci. Technol.* **2011**, *26*, 022002.
- [35] M. L. Lee, J. K. Sheu, S. W. Lin, *Appl. Phys. Lett.* **2006**, *88*, 032103.
- [36] F. Iucolano, F. Roccaforte, F. Giannazzo, V. Raineri, *J. Appl. Phys.* **2008**, *104*, 093706.
- [37] N. Miura, T. Nanjo, M. Suita, T. Oishi, Y. Abe, T. Ozeki, H. Ishikawa, T. Egawa, T. Jimbo, *Solid-State Electron.* **2004**, *48*, 689.
- [38] K. Shiojima, T. Suemitsu, M. Ogura, *Appl. Phys. Lett.* **2001**, *78*, 3636.
- [39] J. Spradlin, S. Doğan, J. Xie, R. Molnar, A. A. Baski, H. Morkoc, *Appl. Phys. Lett.* **2004**, *84*, 4150.
- [40] F. Iucolano, F. Roccaforte, F. Giannazzo, V. Raineri, *J. Appl. Phys.* **2007**, *102*, 113701.
- [41] F. Iucolano, F. Roccaforte, F. Giannazzo, V. Raineri, *Appl. Phys. Lett.* **2007**, *90*, 092119.
- [42] H. Heinke, V. Kirchner, S. Einfeldt, D. Hommel, *Appl. Phys. Lett.* **2000**, *77*, 2145.
- [43] P. Fiorenza, F. Giannazzo, A. Frazzetto, F. Roccaforte, *J. Appl. Phys.* **2012**, *112*, 084501.
- [44] F. Iucolano, F. Roccaforte, A. Alberti, C. Bongiorno, S. Di Franco, V. Raineri, *J. Appl. Phys.* **2006**, *100*, 123706.
- [45] F. Iucolano, F. Roccaforte, F. Giannazzo, V. Raineri, *J. Appl. Phys.* **2008**, *104*, 093706.
- [46] F. Roccaforte, F. La Via, V. Raineri, F. Mangano, L. Calcagno, *Appl. Phys. Lett.* **2003**, *83*, 4181.
- [47] A. M. Witowski, K. Pakuła, J. M. Baranowski, M. L. Sadowski, P. Wyder, *Appl. Phys. Lett.* **1999**, *75*, 4154.
- [48] F. Roccaforte, F. La Via, V. Raineri, R. Pierobon, E. Zanoni, *J. Appl. Phys.* **2003**, *93*, 9137.
- [49] F. Giannazzo, F. Roccaforte, F. Iucolano, V. Raineri, F. Ruffino, M. G. Grimaldi, *J. Vac. Sci. Technol. B* **2009**, *27*, 789.
- [50] B. Ren, M. Liao, M. Sumiya, L. Wang, Y. Koide, L. Sang, *Appl. Phys. Express* **2017**, *10*, 051001.
- [51] P. Reddy, B. Sarkar, F. Kaess, M. Gerhold, E. Kohn, R. Collazo, Z. Sitar, *Appl. Phys. Lett.* **2017**, *110*, 011603.
- [52] H. C. Kang, S. H. Seo, H. W. Jang, D. H. Kim, D. Y. Noh, *Appl. Phys. Lett.* **2003**, *83*, 2139.